

# Numerical simulation of three-dimensional laminar multiple impinging square jets

L.B.Y. Aldabbagh, I. Sezai \*

*Department of Mechanical Engineering, Eastern Mediterranean University, Magusa, 10 Mersin, Turkey*

Received 2 June 2001; accepted 20 January 2002

## Abstract

The flow and heat transfer characteristics of impinging laminar multiple square jets have been investigated numerically through the solution of the three-dimensional Navier–Stokes and energy equations in steady state. The simulations have been carried out for jet-to-jet spacings of  $4D$ ,  $5D$  and  $6D$  and for nozzle exit to plate distances between  $0.25D$  and  $9D$ , where  $D$  is the jet width. The calculated results show that the flow structure of multiple square jets impinging on a heated plate is strongly affected by the jet-to-plate distance. On the other hand, the magnitude of the local maximum Nusselt number at the stagnation point is not affected by jet-to-jet spacing. Moreover, for very small jet-to-plate distances ( $L_z \approx 0.25D$ ), no upwash-fountain flow can form at the collision point, where the jets are merely diverted in the transverse direction. For such rather low nozzle-to-plate distances the wall jet fills the whole gap between the plates where no vortex motion forms around the jets. © 2002 Elsevier Science Inc. All rights reserved.

*Keywords:* Three-dimensional laminar multiple impinging square jets

## 1. Introduction

Impinging jets have found a large number of applications where high rates of convective heat transfer are required. Industrial uses of impinging air jets include tempering of glass, drying of paper and textiles, and the cooling of the metal sheets, microelectronic components and turbine blades. Although such jets yield very high heat transfer coefficients in the stagnation zone the cooling performance drops rapidly away from the impingement zone. For this reason, and to increase the uniformity of the heat flux distribution, jets are often used in arrays. In addition, arrays of jets are used when heating or cooling a variety of industrial products with large surface areas. In such cases the interaction between the jets in the array plays an important role in the cooling performance. The collision of the wall jets after impingement produces a rather complex flow field. Therefore, the study of three-dimensional array of impinging jets may provide some basic understanding, which cannot be predicted by two-dimensional simulations.

The experimental and theoretical investigations on jets are mostly related to turbulent jets. Although many applications involve turbulent jets, laminar jets are also encountered when the fluid is highly viscous or the geometry is miniaturized as in microelectronics.

Hollworth and Dagan (1980) examined experimentally an impinging jet array system with spent fluid exits distributed on the impingement surface, concluding that for the same coolant flow per unit area of target surface, staggered arrays with large jet-to-jet spacings (15 and 20 nozzle diameters) produce higher average heat transfer coefficient than those with small jet-to-jet spacings (5 nozzle diameter). Obot and Trabold (1987) experimentally observed that the degradation in heat transfer with single and dual-exit drainage configurations for arrays of jets, for a given mass flow rate of air, is more pronounced as the jet-to-jet spacings decrease or as the number of jets over a fixed target area increases. The effect of jet-to-jet spacings (4, 6, and 8 nozzle diameter) with low nozzle-to-plate spacings (0.25, 1.0 and 6.0 nozzle diameter) on convective heat transfer coefficient was investigated experimentally by Huber and Viskanta (1994). They used  $3 \times 3$  square arrays of confined axisymmetric turbulent air jets impinging normally onto a heated surface. Their results show that the highest

\* Corresponding author. Fax : +90-392-36-53-715.  
E-mail address: ibrahim.sezai@emu.edu.tr (I. Sezai).

### Nomenclature

$A_x, A_y, A_z$	aspect ratios in $x$ -, $y$ - and $z$ -direction, $L_x/D$ , $L_y/D$ , $L_z/D$	$V$	nondimensional Cartesian velocity, in $y$ -direction ( $v/u_j$ )
$D$	jet width (m)	$W$	nondimensional Cartesian velocity, in $z$ -direction ( $w/u_j$ )
$h$	heat transfer coefficient ( $\text{W}/\text{m}^2 \text{K}$ )	$u, v, w$	Cartesian velocities
$L_x, L_y, L_z$	length of heated surface in $x$ -, $y$ - and $z$ -directions, respectively (m)	$X_n, Y_n$	jet–jet spacing in $x$ - and $y$ -directions, respectively
$k$	thermal conductivity ( $\text{W}/\text{m K}$ )	$X, Y, Z$	nondimensional Cartesian coordinates, $x/D$ , $y/D$ , $z/D$ respectively
$Nu$	local Nusselt number ( $hD/k$ )	$x, y, z$	Cartesian coordinates
$P$	nondimensional pressure ( $p/\rho u_j^2$ )	<i>Greeks</i>	
$p$	pressure ( $\text{N}/\text{m}^2$ )	$\nu$	kinematic viscosity ( $\text{m}^2/\text{s}$ )
$Pr$	Prandtl number ( $\nu/\alpha$ )	$\rho$	density ( $\text{kg}/\text{m}^3$ )
$q_w''$	local convective heat flux at the impingement plate	$\alpha$	thermal diffusivity ( $\text{m}^2/\text{s}$ )
$Re$	jet Reynolds number ( $u_j D/\nu$ )	$\phi$	$U, V, W, P$ , or $T$ field
$T$	nondimensional temperature, $(t - t_j)/(t_w - t_j)$	<i>Subscripts</i>	
$t$	temperature (K)	$j$	jet exit
$u_j$	jet exit velocity (m/s)	$w$	wall
$U$	nondimensional Cartesian velocity, in $x$ -direction ( $u/u_j$ )		

average Nusselt number for a given jet-to-plate distance, as well as the most uniform distribution over the impingement surface, were obtained at jet-to-jet spacing of four nozzle diameters. Also, they report that the average Nusselt number for small jet-to-plate distances (less than one nozzle diameter) increases due to secondary peak formation. The increase in heat transfer due to the secondary peak of the Nusselt number at low jet-to-plate distances (less than one jet diameter) has also been found in single impinging jets. Lytle and Webb (1994) reported a secondary peak of the Nusselt number for a single turbulent impinging jet. The multiple impinging jet array systems with crossflow have been extensively investigated by Metzger et al. (1979); Saad et al. (1980); Kim and Benson (1993); Slayzak et al. (1994) and Barata (1996), particularly with respect to how the geometric arrangement influences the heat-transfer performance. They have found that the cross flow always tends to degrade the heat-transfer performance. The heat-transfer characteristics of single- and dual-exit drainage configurations for arrays of liquid jets impinging normal to a heated isoflux plate, have been studied experimentally by Garrett and Webb (1999). They found that the plate-average heat-transfer coefficient increases for decreasing jet-to-jet spacing. Moreover, the maximum plate average Nusselt number was found at nozzle-to-plate spacing of four jet diameters.

There is a considerable body of literature dealing with flow and heat transfer in laminar arrays of jets. Gardon and Akfirat (1966) carried out an early work to measure the heat transfer coefficients between a flat plate and impinging 2-D slot-jets. They focused on single and ar-

rays of free air jets in laminar and turbulent flow conditions. Kercher and Tabakoff (1970) report from their experiment that the heat transfer for a square array of round air jets impinging perpendicular to a flat surface strongly depends on the jet-to-jet spacing. Moreover, by increasing the jet-to-plate spacing the heat transfer increases without crossflow but decreases with crossflow. Mikhail et al. (1982) numerically studied the flow and heat transfer characteristics of laminar jets issuing from a row of slots and impinging normally on a flat plate. Their results show that the average Nusselt number increases as the nozzle-to-plate spacing decreases. Ichimiya (1991) and Ichimiya and Hosaka (1992) studied experimentally (for laminar and turbulent jets) and numerically (for laminar case only) the characteristics of flow and heat transfer caused by three laminar impinging jets. The laminar simulations were carried out for  $Re = 500$ . Both experimental and numerical results show that a recirculating flow is generated between two nozzles and the position of the maximum heat transfer depends on the flow from the adjacent nozzles and the distance between the nozzle and the impingement surface. The effect of the crossflow which arises in the multiple impingement jet configuration was considered in the laminar numerical work carried out by Al-Sanea (1992). He found that the presence of a crossflow degrades the favourable heat transfer characteristics of impinging jets, and can reduce the nominal Nusselt number by as much as 60%. Seyedein et al. (1994) numerically studied the two-dimensional flow field and heat transfer due to laminar multiple slot jets discharging normally into a converging confined channel. The

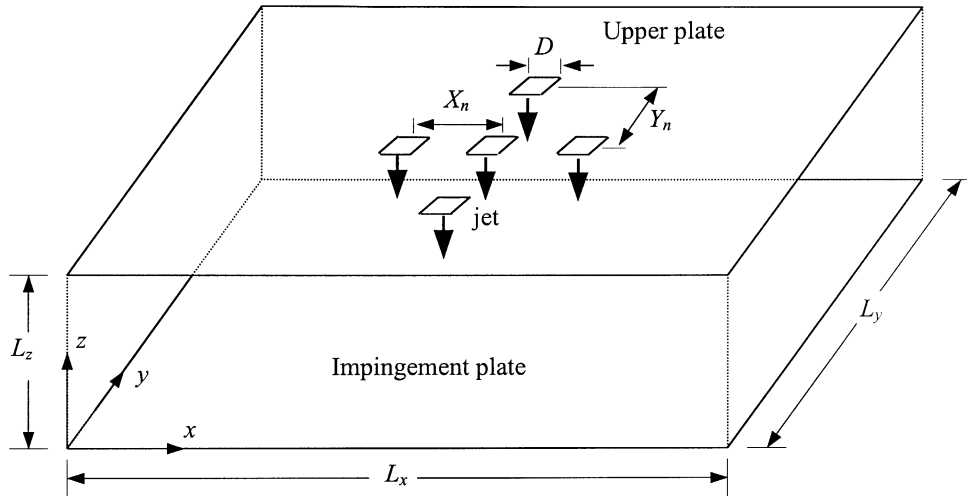


Fig. 1. Definitions of geometric parameters and the coordinate system.

simulations were carried out for jet Reynolds numbers  $600 < Re < 1000$  and for the angle of inclination of the upper surface in the range  $(0^\circ-20^\circ)$ . They found that the inclination of the confined surface levels out the Nusselt number distribution on the impingement surface as a result of exhaust flow acceleration along flow direction. A high degree of uniformity of heat transfer could be obtained at a plate inclination angle of  $10^\circ$ .

Although most industrial applications of jets in industry are in the turbulent regime, the three-dimensional laminar flow structure resulting from a square jet is far from being fully understood. The present work deals with the analysis of a laminar, three-dimensional, square array of five jets impinging on a heated flat surface see (Fig. 1). The structure of the flow field and its effect on the heat transfer characteristics are investigated numerically for Reynolds numbers 100, 200, 300, 400, and 500.

## 2. Computation scheme

The steady-state, three-dimensional, Navier–Stokes and energy equations for incompressible flows in Cartesian coordinates are used for this study. The velocity and length are nondimensionalized by jet-exit velocity and jet width, respectively. The temperature is nondimensionalized by  $(t - t_j)/(t_w - t_j)$ . Buoyancy effects have been neglected.

The nondimensional continuity, momentum and energy equations for laminar flow with constant properties can be written as:

$$\frac{\partial U}{\partial X} + \frac{\partial V}{\partial Y} + \frac{\partial W}{\partial Z} = 0 \quad (1)$$

$$U \frac{\partial U}{\partial X} + V \frac{\partial U}{\partial Y} + W \frac{\partial U}{\partial Z} = -\frac{\partial P}{\partial X} + \frac{1}{Re} \nabla^2 U \quad (2)$$

$$U \frac{\partial V}{\partial X} + V \frac{\partial V}{\partial Y} + W \frac{\partial V}{\partial Z} = -\frac{\partial P}{\partial Y} + \frac{1}{Re} \nabla^2 V \quad (3)$$

$$U \frac{\partial W}{\partial X} + V \frac{\partial W}{\partial Y} + W \frac{\partial W}{\partial Z} = -\frac{\partial P}{\partial Z} + \frac{1}{Re} \nabla^2 W \quad (4)$$

$$U \frac{\partial T}{\partial X} + V \frac{\partial T}{\partial Y} + W \frac{\partial T}{\partial Z} = \frac{1}{RePr} \nabla^2 T \quad (5)$$

Boundary conditions for velocities: the outlet boundary is located far enough downstream for conditions to be substantially developed, accordingly the following conditions are imposed:

$$\frac{\partial U}{\partial X} = \frac{\partial V}{\partial X} = \frac{\partial W}{\partial X} = 0 \quad \text{at } X = 0, X = A_x$$

$$\frac{\partial U}{\partial Y} = \frac{\partial V}{\partial Y} = \frac{\partial W}{\partial Y} = 0 \quad \text{at } Y = 0, Y = A_y$$

All walls are stationary and impervious therefore the no-slip boundary condition is used for the top and bottom solid walls except the  $W$  velocity at the jets exit cross-section at the top wall, where it was set to be equal to unity and, hence,  $U = V = W = 0$  at  $Z = 0, Z = A_z$  except at nozzle exit,  $U = V = 0, W = -1$  at nozzle exit.

Boundary conditions for temperature are as follows: if the fluid exits the domain the first derivative of temperature is set to zero and if the fluid flows from the surroundings into the domain then the fluid temperature is set to surrounding temperature. That is

$$\text{At } X = 0 \quad \begin{aligned} \frac{\partial T}{\partial X} &= 0 \quad \text{for } U < 0 \\ T &= 0 \quad \text{for } U > 0 \end{aligned}$$

$$\text{At } X = A_x \quad \begin{aligned} \frac{\partial T}{\partial X} &= 0 \quad \text{for } U > 0 \\ T &= 0 \quad \text{for } U < 0 \end{aligned}$$

$$\text{At } Y = 0 \quad \begin{aligned} \frac{\partial T}{\partial Y} &= 0 \quad \text{for } V < 0 \\ T &= 0 \quad \text{for } V > 0 \end{aligned}$$

$$\text{At } Y = A_y \quad \begin{cases} \frac{\partial T}{\partial Y} = 0 & \text{for } V > 0 \\ T = 0 & \text{for } V < 0 \end{cases}$$

Adiabatic boundary conditions are imposed on the top wall, except at the nozzle exit cross-section where it was set to be equal to that of ambient. The bottom wall is set to a higher temperature than the ambient,

$$\text{At } Z = 0 \quad T = 1$$

$$\text{At } Z = A_z \quad \begin{cases} \frac{\partial T}{\partial Z} = 0 & \text{except at nozzle exit} \\ T = 0 & \text{at nozzle exit.} \end{cases}$$

### 3. Method of solution

The governing equations are discretized by using the finite-volume method in staggered, nonuniform grids. The grids are generated such that denser grid clustering is obtained at the center of the jets-exit cross-section in the  $x$  and  $y$ -direction and increase far from the center of the jets. The solution domain in the  $x$  and  $y$ -directions has  $L_x = L_y = 35D$ . In the  $z$ -direction a sine function distribution is employed, yielding denser grids near the top and near the impingement plate. The difference between the results obtained for the average Nusselt number with  $171 \times 171 \times 51$  grids and  $151 \times 151 \times 41$  is 0.63%, while the difference between  $151 \times 151 \times 41$  and  $131 \times 131 \times 31$  grids is 2%. Hence, all calculations are performed with  $151 \times 151 \times 41$  grids. The QUICK scheme (Leonard, 1979) with ULTRA-SHARP flux limiting strategy (Leonard and Mokhtari, 1990; Leonard and Drummond, 1995) was used to calculate the convection of a scalar term ( $\phi$ ) at a control volume face. The extra neighboring points resulting from the application of QUICK scheme is written as the sum of the upwind face value plus a correction term involving the values from the previous iteration. The correction term is added to the source term in accordance with deferred correction procedure (Leonard and Drummond, 1995) so that the numerical stability is increased, while keeping the seven diagonal structure of the coefficient matrix. The Bi-CGSTAB (Van der Vorst, 1989) iterative method with SSOR preconditioning (Saad, 1996) is applied to the pressure and energy equations in the sequential procedure of the SIMPLEX (Van Doormaal and Raithby, 1984) algorithm. An under-relaxation factor of 0.8 for  $Re = 100$  and 200 and 0.7 for  $Re = 300, 400$  and 500

is used for momentum and energy equations in all calculations. Iterations are continued until the second norm of the residuals for all equations are reduced below  $10^{-6}$ , where no significant variations are observed at this residual level.

## 4. Results and discussion

Air is used as the working, fluid, having a Prandtl number of 0.71. The analysis is performed for Reynolds numbers between 100 and 500 and aspect ratios,  $A_z$ , between 0.25 and 9. Center-to-center distance values between the jets used are:  $4D, 5D$  and  $6D$ , where  $X_n = Y_n$  is used for all the cases. The cross-section of the nozzles is taken to be square and the velocity distribution at the exit of the nozzles is assumed to have a flat profile.

### 4.1. Flow structure

Fig. 2 shows the projection of flow lines of the predicted velocity field on the mid vertical  $x$ - $z$  plane, for a plate-to-plate distance of one jet width, with  $X_n = 5$  and  $Re = 500$ . The projection of flow lines on a  $x$ - $z$  plane are obtained from the  $U$  and  $W$  components of the velocity vectors on that plane. At the impingement plane, wall jets are formed spreading radially in all directions. At the collision front of the wall jets an upwash-fountain flow is formed between each two impinging jets. Upon impingement of the upwash-fountain on the top wall, an upper wall jet is formed which is diverted along the radial directions. As soon as the jets exit from the nozzles, the fluid is dragged radially towards the jets from the surrounding. As a result a toroidal vortex is formed around each of the jets. The evolution of the entrainment vortex and wall jets is illustrated in Fig. 3 through a projection of the flow lines on different horizontal planes. Fig. 3a corresponds to a horizontal plane where upper wall jets are formed as upwash-fountains impinge on the top plate. The upwash-fountain flows are directed towards the jets near the top plate. The wall jet on the bottom plane starts forming at  $Z = 0.3$  (Fig. 3c) as a result of jet impingement on the bottom plate. Further downstream, at  $Z = 0.1$ , the wall jets are more prominent (Fig. 3d). The wall jet of the central jet spreads outward along the diagonal directions in between the wall jets, which are formed as the surrounding jets impinge on the bottom plate. The wall jets are separated from each other along the ground plane by stagnation

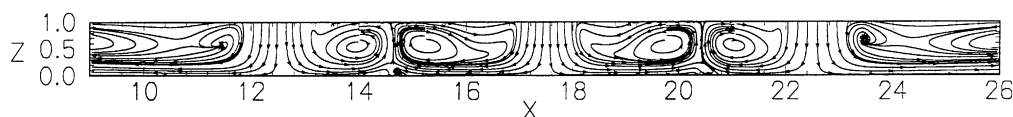


Fig. 2. Projection of flow lines for  $Re = 500, A_z = 1$  and  $X_n = 5$  on mid  $x$ - $z$  plane at  $Y = 17.5$ .

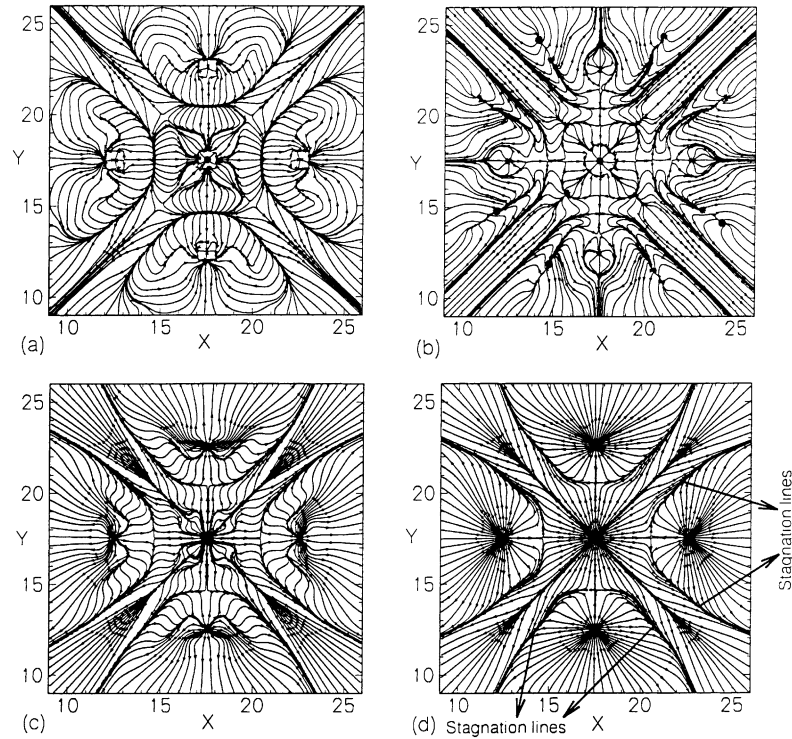


Fig. 3. Projection of flow lines for  $Re = 500$ ,  $A_z = 1$  and  $X_n = 5$  at horizontal cross-sections of (a)  $Z = 0.9$ , (b)  $Z = 0.5$ , (c)  $Z = 0.3$  and (d)  $Z = 0.1$ .

lines or dividing lines everywhere between each impingement jet, containing a stagnation point. A carpet plot of the vertical component of the velocity at the horizontal section at  $Z = 0.5$  is shown in Fig. 4. For this rather low plate-to-plate spacing, the interaction of the jet with the lower plate produces four peaks at the four corners of each jet cross-section. The off-center peaks of the jet velocity have also been observed in incompress-

ible turbulent unbounded single jet flows issuing from rectangular nozzles by Sfeir (1979); Tsuchiya et al. (1986) and Quinn (1991) and in laminar rectangular single jet flows with small jet to wall distances (Sezai and Mohamad, 1999). The formation of the off-center velocity peaks near the edges of the jet is generally attributed to the fluid acceleration out of the stagnation region due to continuity requirements (Viskanta, 1993;

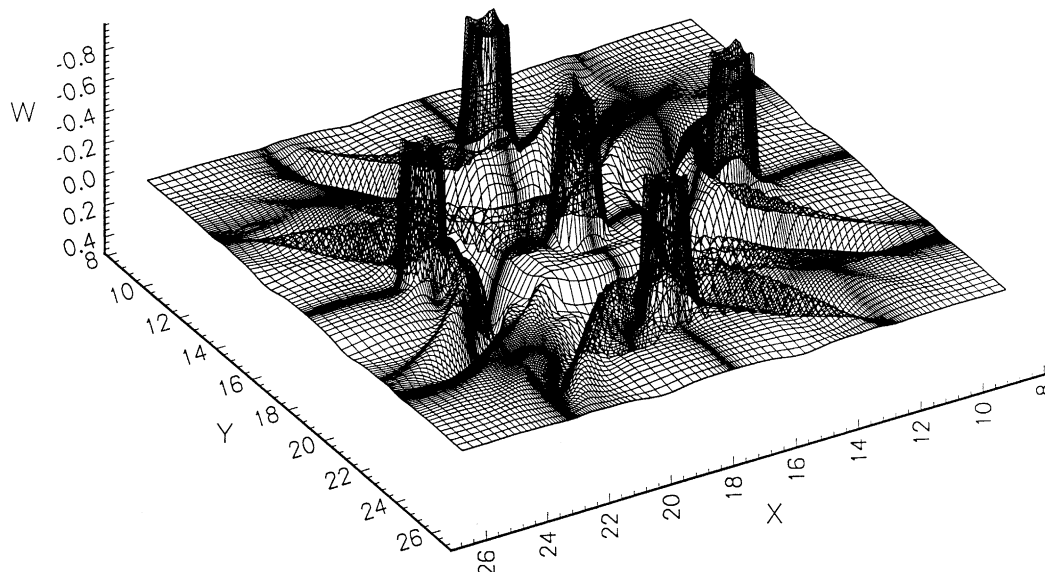


Fig. 4. The three-dimensional plots of the  $W$ -velocity for  $Re = 500$ ,  $A_z = 1$  and  $X_n = 5$  at horizontal cross-section  $Z = 0.5$ .

Lytle and Webb, 1994; Webb and Ma, 1995). On the other hand, Chatterjee and Deviprasath (2001) attribute the formation of off-center velocity peaks to the distortion in the velocity distribution at the jet exit plane as a result of diffusion of vorticity, which is generated at the impingement surface. However, in the present study the jet exit velocity is arbitrarily fixed to be uniform. For such a flat velocity distribution at the exit plane it has been found that (Sezai and Mohamad, 1999) the impinging flow has a strong vorticity near the impingement plate and that the vorticity weakens away from the impingement plate. It seems that the vorticity generated at the impinging surface diffuses upstream and affects the originally flat velocity distribution, producing the four off-center velocity peaks.

The variation of the vertical velocity component with vertical distance from the jet nozzles is shown in Fig. 5. The off-center velocity peaks start forming after issuing from the nozzle exit. The difference between the peak and the jet centerline velocity reaches a maximum at  $Z = 0.3$  and then gradually levels off at closer distances to the impingement plane. As Sezai and Mohamad (1999) have suggested, the off-center velocity peaks are formed by the diffusion of vorticity along wall jets, as the jet impinges on the plate.

Fig. 6a–d shows the projection of flow lines on the mid vertical  $x$ – $z$  plane for  $Re = 100$ ,  $X_n = 5$  and  $A_z = 2$ , 4, 6 and 8. For the rather small nozzle-to-plate spacings of  $2D$  and  $4D$  (Fig. 6a and b) the upwash-fountain flows impinge on the top plate, forming wall jets at that plane.

As the separation between the plates increases the upwash-fountain flows cannot reach the top plate, and as a result the upper wall jets cannot form (Fig. 6c and d). The peripheral vortices stretch along the vertical direction and for  $A_z = 8$  the peripheral vortex around the central jet is divided into two co-rotating vortices. The formation of the peripheral vortices and the wall jets for  $A_z = 6$  is illustrated in Fig. 7, using the projection of flow lines at different horizontal planes. The fluid is dragged radially towards the jets from the surrounding with complex flow patterns as shown in Fig. 7a–c. At elevations closer to the bottom plate, the flow pattern is characterized by the wall jets, which are separated from each other at the collision front (Fig. 7d). The vertical component of the velocity of each jet has a single peak, which is located at the center of the jet.

At lower nozzle-to-plate spacings the upwash flow may disappear completely. Fig. 8 shows the projection of flow lines on the mid vertical plane for a nozzle-to-plate spacing of  $0.25D$  for  $Re = 200$  and  $X_n = 5$ . The wall jet fills the whole gap between the plates, where no recirculatory motion can form between the jets at this small separation distance. No off-center velocity peaks of the jet profile were found for nozzle-to-plate distance lower than one.

#### 4.2. Heat transfer

The local convection heat transfer coefficient is defined as

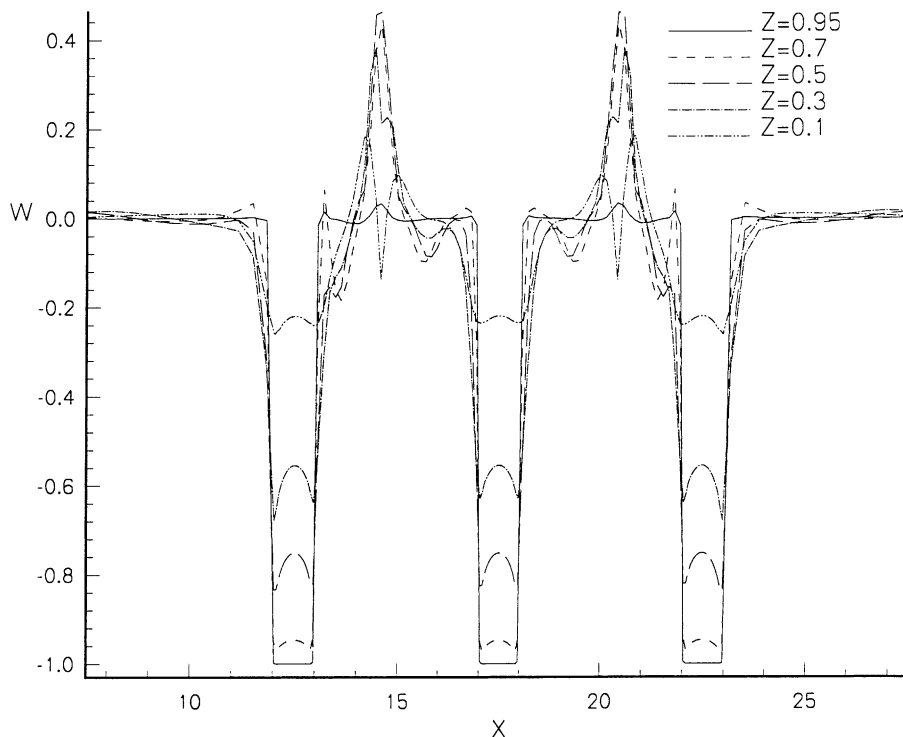


Fig. 5. Variation of  $W$ -velocity with  $X$  for  $Re = 500$ ,  $A_z = 1$  and  $X_n = 5$  at different horizontal cross-section.

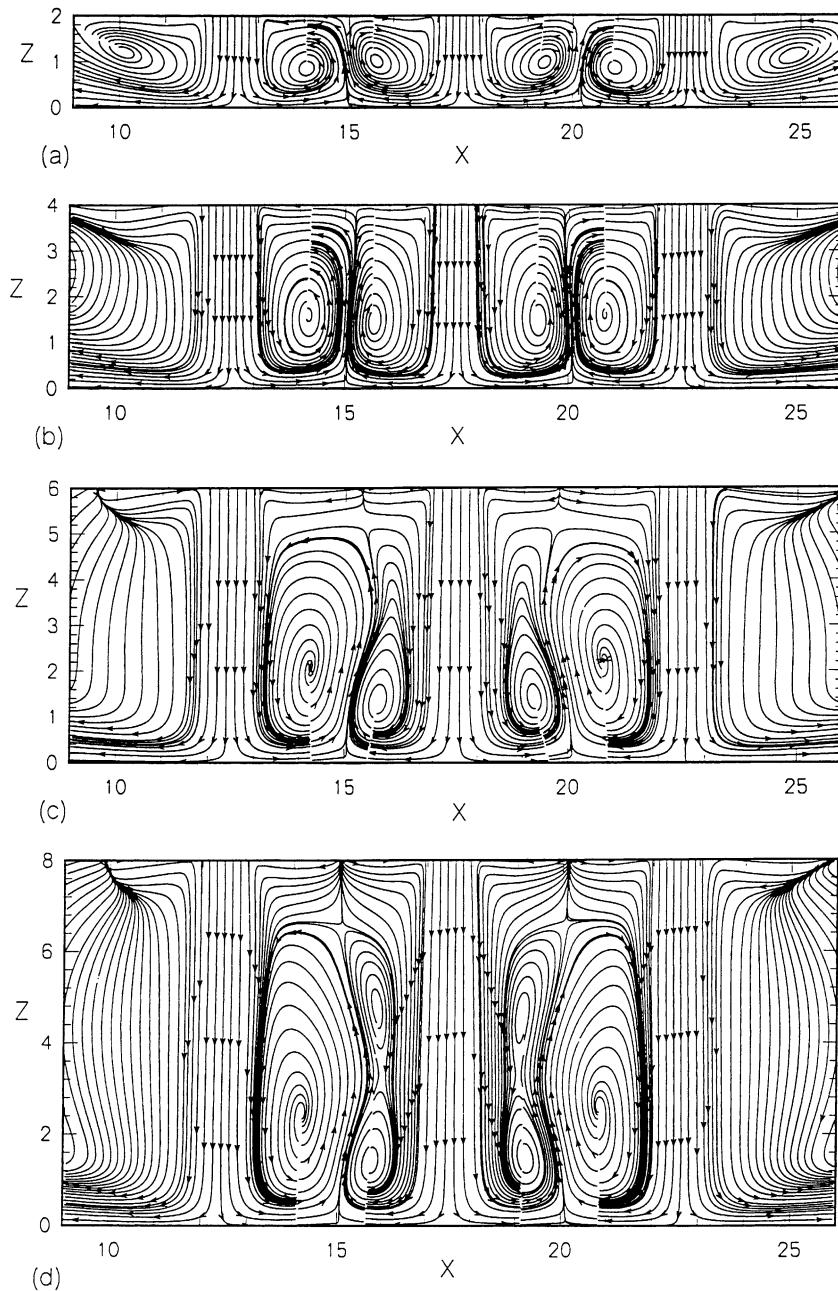


Fig. 6. Projection of flow lines on mid  $x$ - $z$  plane for  $Re = 100$  and  $X_n = 5$  at jet-to-plate spacing (a)  $A_z = 2$ , (b)  $A_z = 4$ , (c)  $A_z = 6$  and (d)  $A_z = 8$ .

$$h = \frac{q_w''}{t_w - t_j} \quad (6)$$

and the local Nusselt number is defined in terms of the jet width,  $D$ , as

$$Nu = \frac{hD}{k} \quad (7)$$

where it is also equal to the nondimensional heat flux and calculated from  $Nu = \partial T / \partial Z$ . The contour plots of the local Nusselt number for  $Re = 500$ ,  $X_n = 5$  and  $A_z = 1$  is shown in Fig. 9 corresponding to the case

shown in Figs. 2–4. The jet stagnation areas are clearly distinguishable as local high Nusselt number regions. The heat transfer decreases steeply away from the stagnation points. However the decrease in local Nusselt number at the stagnation point becomes smooth at lower Reynolds numbers. The four off-center peaks in the Nusselt number for each jet is consistent with the jet velocity profile shown in Fig. 4, which indicate that the jet velocity distribution plays a significant role in impingement cooling. The formation of four off-center peak of the Nusselt number at the core of each jet was also reported in laminar square single jet flows by Sezai

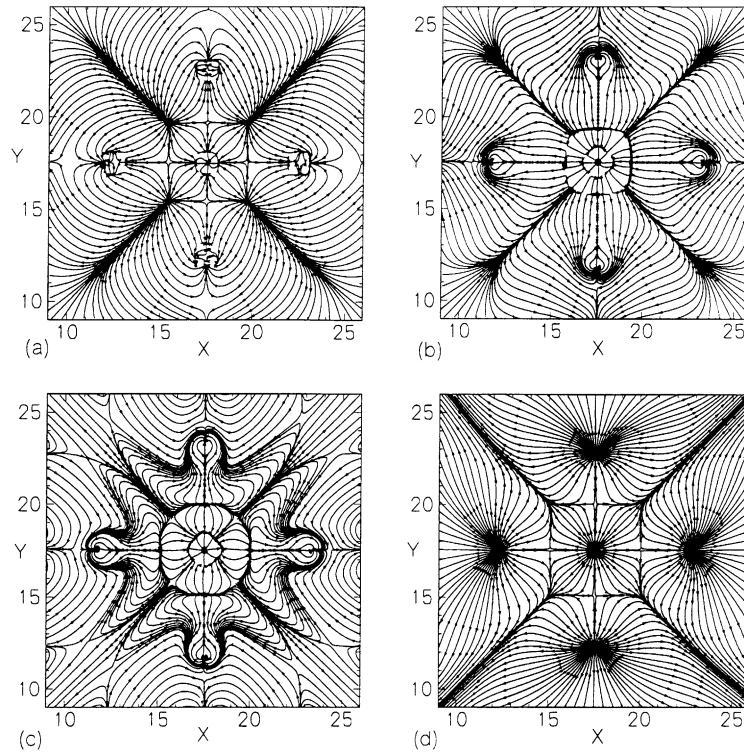


Fig. 7. Projection of flow lines for  $Re = 100$ ,  $A_z = 6$  and  $X_n = 5$  on horizontal cross-section at (a)  $Z = 5.4$ , (b)  $Z = 4.2$ , (c)  $Z = 3$  and (d)  $Z = 0.6$ .



Fig. 8. Projection of flow lines on mid  $x-z$  plane for  $Re = 200$ ,  $A_z = 0.25$  and  $X_n = 5$ .

and Mohamad (1999). However, no such off-center peaks are observed for the rather small nozzle-to-plate distance of  $L_z = 0.25D$ . The secondary peak in Nusselt number for small nozzle-to-plate distances  $L_z = 0.25D$ , mentioned by Huber and Viskanta (1994) on a  $3 \times 3$  square turbulent jet array and for single turbulent jet by Lytle and Webb (1994) and Oyakawa et al. (1997), is not found for the rather low nozzle-to-plate spacing and the Reynolds numbers investigated in this paper. The effect of jet-to-jet spacing,  $X_n$ , on the variation of local Nusselt number along  $x$ -direction at the mid-section is shown in Fig. 10a–c for  $Re = 300$  and  $A_z = 0.25, 1$  and  $2$ . It is observed that the magnitude of the maximum Nusselt number is not affected by the jet-to-jet spacing. For all cases investigated in this paper, the local Nusselt numbers at the stagnation points have been found to be the same in magnitude as those of the single square jets obtained by Sezai and Mohamad (1999). Moreover, the stagnation Nusselt number increases as the nozzle-to-plate distance decreases. The rate of change in the stagnation Nusselt number is higher at closer nozzle-to-plate spacings (Fig. 10a). For the smallest nozzle-

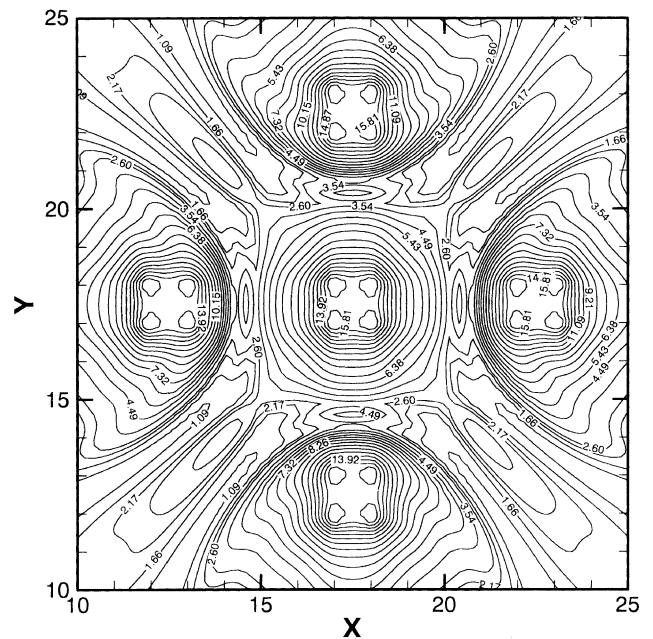


Fig. 9. The contour plot of the Nusselt number for  $Re = 500$ ,  $A_z = 1$  and  $X_n = 5$ .

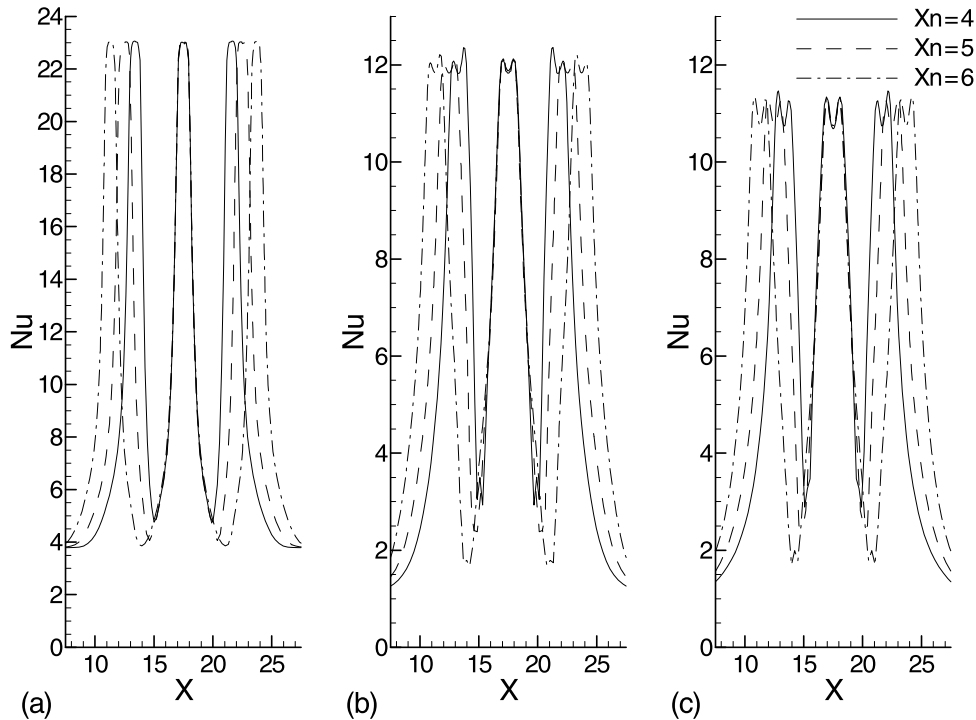


Fig. 10. Effect of jet-to-jet spacing on Nusselt number variation for  $Re = 300$  and (a)  $A_z = 0.25$ , (b)  $A_z = 1$  and (c)  $A_z = 2$ .

to-plate spacing investigated, ( $L_z \approx 0.25D$ ) the Nusselt number in the region far away the impingement zone is much higher than that of the other nozzle-to-plate spacings due to the higher wall jet velocities attained.

## 5. Conclusion

A three-dimensional numerical study is used to determine the flow and heat transfer characteristics of multiple impinging jets of square cross-section. The results indicate a rather complex flow field with the formation of a peripheral vortex around each jet and an upwash-fountain flow at the collision point of the jets. The size and location of any peripheral vortex depends on the nozzle-to-plate spacings. However, at very small nozzle-to-plate distances ( $L_z \approx 0.25D$ ), no upwash-fountain flow can form at the collision point, where the jets are diverted along the transverse directions. At this nozzle-to-plate distance wall jets may fill the whole plate-to-plate spacing so that no vortex motion can form around the jets. Moreover, the Nusselt number, far from the impingement zone is much higher than at larger nozzle-to-plate spacings due to higher wall jet velocities. In addition, no secondary peak of the Nusselt number was found for this small separation distance.

Heat transfer is strongly affected by the jet-to-plate spacings. However, the magnitude of the maximum Nusselt number is not affected by the jet-to-jet spacing. For a nozzle-to-plate spacing of one and two nozzle

widths, the uniform jet velocity profile at the nozzle exit is transformed into a nonuniform profile having four off-center velocity peaks downstream of the nozzles. These peaks result in the formation of four off-center peaks in the Nusselt number profile at the impingement plate.

## References

- Al-Sanea, S., 1992. A numerical study of the flow and heat transfer characteristics of an impinging laminar slot-jet including crossflow effects. *Int. J. Heat Mass Transfer* 35 (10), 2501–2513.
- Barata, J.M.M., 1996. Fountain flows produced by multiple impinging jets in a crossflow. *AAIA J.* 34 (12), 2523–2530.
- Chatterjee, A., Deviprasath, L.J., 2001. Heat transfer in confined laminar axisymmetric impinging jets at small nozzle-plate distances: the role of upstream vorticity diffusion. *Numer. Heat Transfer, Part A* 39, 777–800.
- Gardon, R., Akfirat, J.C., 1966. Heat transfer characteristics of impinging two-dimensional air jets. *ASME J. Heat Transfer* 88, 101–108.
- Garrett, K., Webb, B.W., 1999. The effect of drainage configuration on heat transfer under an impinging liquid jet array. *ASME J. Heat Transfer* 121, 803–810.
- Hollworth, B.R., Dagan, L., 1980. Arrays of impinging jets with spent fluid removal through vent holes on the target surface, Part 1: Average heat transfer. *J. Eng. Power* 102, 994–999.
- Huber, A.M., Viskanta, R., 1994. Effect of jet-jet spacing on convective heat transfer to confined, impinging arrays of axisymmetric air jets. *Int. J. Heat Mass Transfer* 37 (18), 2859–2869.
- Ichimiya, K., 1991. Numerical estimation on impingement heat transfer caused by confined three slot jets. *Proc. 4th Int. Symp. Transport Phenomena in Heat and Mass Transfer*, 456–467.

- Ichimiya, K., Hosaka, N., 1992. Experimental study of heat transfer characteristics due to confined impinging two-dimensional jets. *Exp. Thermal Fluid Sci.* 5, 803–807.
- Kercher, D.M., Tabakoff, W., 1970. Heat transfer by a square array of round air jets impinging perpendicular to a flat surface including the effect of spent air. *J. Eng. Power* 10, 73–82.
- Kim, S.W., Benson, T.J., 1993. Fluid flow of a row of jets in crossflow—a numerical study. *AIAA J.* 31 (5), 806–811.
- Leonard, B.P., 1979. A stable and accurate convective modelling procedure based on quadratic upstream interpolation. *Comput. Method Appl. Mech. Eng.* 19, 59–98.
- Leonard, B.P., Mokhtari, S., 1990. Beyond first order upwinding: the ULTRA-SHARP alternative for nonoscillatory steady-state simulation of convection. *Int. J. Numer. Meth. Eng.* 30, 729–766.
- Leonard, B.P., Drummond, J.E., 1995. Why you should not use 'Hybrid,' 'Power Law' or related exponential schemes for convective modelling. There are much better alternatives. *Int. J. Numer. Meth. Fluids* 20, 421–442.
- Lytle, D., Webb, B.W., 1994. Air jet impingement heat transfer at low Nozzle-plate spacings. *Int. J. Heat Mass Transfer* 37, 1687–1697.
- Metzger, D.E., Florschuetz, L.W., Takeuchi, D.I., Behee, R.D., Berry, R.A., 1979. Heat transfer characteristics for inline and staggered arrays of circular jets with crossflow of spent air. *J. Heat Transfer* 101, 526–531.
- Mikhail, S., Morcos, S.M., Abou-Ellail, M.M.M., Ghaiy, W.S., 1982. Numerical prediction of flow field and heat transfer from a row of laminar slot jets impinging on a flat plate. *Proc. 7th Int. Heat Transfer Conf.* 3, 377–382.
- Obot, N.T., Trabold, T.A., 1987. Impingement heat transfer within arrays of circular jets: Part 1—Effects of minimum intermediate, and complete crossflow for small and large spacings. *ASME J. Heat Transfer* 109, 872–879.
- Oyakawa, K., Matsuda, S., Yaga, M., 1997. Study on impingement heat transfer with non-circular jets using infrared imaging method. *Proc. 4th world Conf. Experiment heat transfer, fluid mechanics and thermodynamics*, Brussels, 1807–1814.
- Quinn, W.R., 1991. Passive near-field mixing enhancement in rectangular jet flows. *AIAA J.* 29, 515–519.
- Saad, N.R., Mujumdar, A.S., Abdelmessah, W., Douglas, W.J.M., 1980. Local heat transfer characteristics for staggered arrays of circular impinging jets with crossflow of spent air. *ASME Paper* 80-HT-23.
- Saad, Y., 1996. *Iterative Methods for Sparse Linear Systems*. PSW Publ. Co., Boston.
- Seyedein, S.H., Hasan, M., Mujumdar, A.S., 1994. Laminar flow and heat transfer from multiple impinging slot jets with an inclined confinement surface. *ASME J. Heat Transfer* 37 (13), 1867–1875.
- Sezai, I., Mohamad, A.A., 1999. 3-D simulation of laminar rectangular impinging jets, flow structure and heat transfer. *ASME J. Heat Transfer* 121, 50–56.
- Sfeir, A., 1979. Investigation of three-dimensional turbulent rectangular jets. *AIAA J.* 17, 1055–1060.
- Slayzak, S.J., Viskanta, R., Incropera, F.P., 1994. Effect of interaction between adjacent free surface planar jets on local heat transfer from the impingement surface. *Int. J. Heat Mass Transfer* 37 (2), 269–282.
- Tsuchiya, Y., Horikoshi, C., Sato, T., 1986. On the spread of rectangular jets. *Exp. Fluids* 4, 1197–1204.
- Van der Vorst, H.A.V., 1989. BICGSTAB: A fast and smoothly converging variant of Bi-CG for the solution of non-symmetric linear systems. *SIAM J. Sci. Statist. Comput.* 10, 1174–1185.
- Van Doormaal, J.P., Raithby, G.D., 1984. Enhancements of the SIMPLE method for predicting incompressible fluid flows. *Numer. Heat Transfer* 7, 147–163.
- Viskanta, R., 1993. Heat transfer to impinging isothermal gas and flame jets. *Exp. Thermal Fluid Sci.* 6, 111–134.
- Webb, B.W., Ma, C.F., 1995. Single phase liquid jet impingement heat transfer. *Adv. Heat Transfer* 26, 105–217.